

DAG Learning from Zero-Inflated Count Data Using Continuous Optimization

Noriaki Sato

The Institute of Medical Science, The University of Tokyo

Marco Scutari

Istituto Dalle Molle di Studi sull'Intelligenza Artificiale (IDSIA)

Shuichi Kawano

Faculty of Mathematics, Kyushu University

Rui Yamaguchi

Division of Cancer System Biology, Aichi Cancer Center Research Institute

Division of Cancer Informatics, Nagoya University Graduate School of Medicine

Seiya Imoto

The Institute of Medical Science, The University of Tokyo

Abstract

We address network structure learning from zero-inflated count data by casting each node as a zero-inflated generalized linear model and optimizing a smooth, score-based objective under a directed acyclic graph constraint. Our Zero-Inflated Continuous Optimization (ZICO) approach uses node-wise likelihoods with canonical links and enforces acyclicity through a differentiable surrogate constraint combined with sparsity regularization. ZICO achieves superior performance with faster runtimes on simulated data. It also performs comparably to or better than common algorithms for reverse engineering gene regulatory networks. ZICO is fully vectorized and mini-batched, enabling learning on larger variable sets with practical runtimes in a wide range of domains.

Keywords: Directed Acyclic Graph, Continuous Optimization, Gene Regulatory Networks

1. Introduction

Learning structural dependencies from observational data is a central problem in statistics and machine learning. Structural estimation methods include score-based, constraint-based, and hybrid methods that combine both (Schmidt et al., 2007). In recent years, score-based continuous optimization methods such as NOTEARS, GOLEM, and DAGMA have been developed and increasingly applied to a wide range of problems (Nazaret et al., 2024; Ng et al., 2020; Zheng et al., 2018; Bello et al., 2022). These approaches transform the combinatorial problem of searching over directed acyclic graphs (DAGs) into a continuous optimization problem with differentiable constraints, thereby enabling the use of efficient gradient-based solvers and principled regularization to control model complexity.

Structure learning methods specific to count or zero-inflated count datasets, found in various domains such as medicine and biology, have also been developed. For learning DAGs from count data, Park and Raskutti (2015) proposed a method based on overdispersion scoring. Choi et al. (2020) proposed a zero-inflated Poisson Bayesian network utilizing the Poisson distribution. Choi

and Ni (2023) then developed a state-of-the-art model, ZiGDAG, using hypergeometric distributions and score-based hill-climbing or Tabu greedy search algorithms. This model demonstrates robust performance on simulated data and enables recovery of biologically relevant gene regulatory networks (GRN) from single-cell transcriptomics (SCT) data. Yu et al. (2023) proposed ZiDAG, a DAG learning method built upon earlier hurdle graphical models (McDavid et al., 2019).

These important models are useful for learning DAGs from possibly zero-inflated count data. However, the computational cost of greedy search algorithms can be substantial. In such cases, continuous optimization methods offer significant advantages due to their scalability. In this work, we develop ZICO (Zero-Inflated Continuous Optimization). This DAG learning approach incorporates the log-likelihood derived from node-wise zero-inflated negative binomial (ZINB) or Poisson (ZIP) models together with DAG constraints, using efficient optimization. Compared with state-of-the-art algorithms for structure learning from zero-inflated count data, ZICO demonstrates superior performance with faster runtimes, making it applicable to a wide range of domains.

2. Methods

2.1. Preliminaries

Bayesian networks are a class of graphical models defined over a DAG $G = (V, E)$ with vertex set $V = \{1, \dots, d\}$ and edge set $E \subseteq V \times V$ (Koller and Friedman, 2009). Each vertex $j \in V$ corresponds to a random variable X_j and $Pa(j)$ denotes its parents. Bayesian networks encode the conditional independencies among nodes, leading to the probability factorization

$$p(X_1, \dots, X_d) = \prod_{j=1}^d p(X_j | X_{Pa(j)}).$$

2.2. Proposed Model Architecture

We address the DAG learning problem for zero-inflated count data by formulating the zero-inflated structural equation model underlying ZICO. Each variable $X_j, j = 1, 2, \dots, d$ in the observational count data $X \in \mathbb{N}_0^{n \times d}$ follows a ZINB distribution conditional on its parents,

$$X_j | X_{Pa0(j)}, X_{Pa1(j)} \sim \text{ZINB}(\pi_j(X_{Pa0(j)}), \mu_j(X_{Pa1(j)}), r_j),$$

with link functions:

$$\text{logit}(\pi_j(x)) = \gamma_j + x^T w_j^{(0)} \quad \text{and} \quad \log(\mu_j(x)) = \delta_j + x^T w_j^{(1)},$$

where $w_j^{(0)}, w_j^{(1)} \in \mathbb{R}^d$ are the weights for node j in the zero and count components, γ_j, δ_j are intercepts, and $r_j > 0$ is a dispersion parameter in the negative binomial (NB) distribution. $\pi_j(X_{Pa0(j)})$ is the zero-inflation probability for variable j , and $\mu_j(X_{Pa1(j)})$ is the conditional mean of the NB count component for variable j . The resulting node-wise log-likelihood naturally separates zeros due to a structural process from the sampling zeros arising under an NB count model. Its expression for sample i and node j is

$$\ell_{ij} = \begin{cases} \log(1 - \pi_{ij}) + \pi_{ij} p_{ij}^{r_j} & (x_{ij} = 0) \\ \log \pi_{ij} + \log \Gamma(x_{ij} + r_j) - \log \Gamma(r_j) - \log \Gamma(x_{ij} + 1) \\ \quad + r_j \log p_{ij} + x_{ij} \log(1 - p_{ij}) & (x_{ij} > 0) \end{cases}$$

where $\pi_{ij} = \text{sigmoid}(\gamma_j + x_i^\top w_j^{(0)})$, $p_{ij} = \frac{r_j}{r_j + \mu_{ij}}$, and $\mu_{ij} = \exp(\delta_j + x_i^\top w_j^{(1)})$.

We additionally consider the ZIP model, in which each node follows a ZIP conditional distribution with the same link functions for the zero and count components:

$$X_j | X_{\text{Pa}0(j)}, X_{\text{Pa}1(j)} \sim \text{ZIP}(\pi_j(X_{\text{Pa}0(j)}), \mu_j(X_{\text{Pa}1(j)})),$$

where $\pi_j(X_{\text{Pa}0(j)})$ is the zero-inflation probability for variable j and $\mu_j(X_{\text{Pa}1(j)})$ is the conditional mean of the Poisson (or count) component for variable j . The node-wise ZIP log-likelihood for sample i and node j is

$$\ell_{ij} = \begin{cases} \log((1 - \pi_{ij}) + \pi_{ij}e^{-\mu_{ij}}) & (x_{ij} = 0) \\ \log \pi_{ij} + x_{ij} \log \mu_{ij} \\ -\mu_{ij} - \log \Gamma(x_{ij} + 1) & (x_{ij} > 0) \end{cases}.$$

We minimize the average negative log-likelihood (NLL) for both models. We compute it fully in the log domain in both ZIP and ZINB models using the log-gamma, log-sum-exp, and softplus link functions, ensuring finite scores even when $\pi \rightarrow 1$ or $\mu \rightarrow 0$ for numerical stability (Cui and Wang, 2023).

Let $W_0 = [w_1^{(0)}, w_2^{(0)}, \dots, w_d^{(0)}]$ and $W_1 = [w_1^{(1)}, w_2^{(1)}, \dots, w_d^{(1)}]$ denote the coefficient matrices for the zero and count components, respectively. We enforce acyclicity on W_0 and W_1 separately. The acyclicity is imposed via a log-determinant-based function of an M-matrix transformation of the weighted adjacency matrix, introduced in DAGMA, as follows:

$$h_{\text{ldet}}^s(W_k) = -\log \det(sI - W_k \circ W_k) + d \log s, \quad (k = 0, 1)$$

where $s > 0$ indicates the log-determinant parameter and \circ denotes the Hadamard product.

3. Objective Function and Continuous Optimization

Let $\Theta = \{W_0, W_1, \gamma, \delta, r\}$. To complete our ZICO proposal, we define the following objective with respect to Θ :

$$\begin{aligned} \min_{\Theta} \mu & \left(-\frac{1}{n} \sum_{i=1}^n \sum_{j=1}^d \ell_{ij} + \lambda_{\text{group}} \sum_{j=1}^d \sum_{\substack{k=1 \\ k \neq j}}^d \|((W_0)_{kj}, (W_1)_{kj})\|_2 \right) \\ & + h_{\text{ldet}}^s(W_0) + h_{\text{ldet}}^s(W_1) + \lambda_{\text{align}} \|W_0 - W_1\|_F^2. \quad (1) \end{aligned}$$

The Frobenius-norm penalty $\lambda_{\text{align}} \|W_0 - W_1\|_F^2$ on the adjacency matrices (for both ZINB and ZIP) encourages the alignment between W_0 and W_1 . Following the central-path approach used in DAGMA, the multiplier $\mu > 0$ is gradually decreased during training at specified epoch intervals using a decay parameter α .

An optional elementwise group- ℓ_1 penalty with nonnegative weight $\lambda_{\text{group}} \geq 0$ is applied with a cosine-annealed warm-up schedule. Specifically, the effective regularization at epoch t is

$$\lambda_{\text{eff}}(t) = \frac{\lambda_{\text{group}}}{2} (1 - \cos(\min\{1, t/\text{warm}\} \pi)),$$

where $warm$ controls the length of the warm-up period. This schedule gradually increases the regularization strength from 0 to λ_{group} , dealing with early-training instability.

We use AdamW with gradient clipping (Loshchilov and Hutter, 2019) for solving (1) to learn DAGs using ZICO. To scale to large n , we compute the NLL on mini-batches $B \subseteq \{1, \dots, n\}$ of size $|B|$:

$$\text{NLL}_B = -\frac{1}{|B|} \sum_{i \in B} \sum_{j=1}^d \ell_{ij}.$$

By restricting training to the parameters in W_1 alone, the model reduces naturally to an NB or Poisson formulation (i.e., without the zero-inflation component). The optimization returns two weighted adjacency matrices (W_0, W_1) in the ZINB or ZIP case, and W_1 in the NB or Poisson case.

4. Experiments

4.1. Simulated Data

We generated synthetic datasets with D nodes and a sample size of $N = 500$. First, the true DAGs were sampled under the Erdős-Renyi (ER) and Barabasi-Albert (BA) models, with an edge probability of 0.25 for ER and expected number of three edges per node in BA (Csardi and Nepusz, 2006, Python igraph library).

Once the network structure was determined, we sampled the model parameters. For edges presented in the DAG, coefficients for the zero-inflation component were randomly drawn from a $U(0.5, 2)$. In contrast, coefficients for the mean component were drawn from a $U(-2, -0.5)$. In addition, intercept terms for the zero-inflation component were sampled from a $N(1.5, 0.2)$. In contrast, intercept terms for the mean component were sampled from a $N(1.5, 0.2)$. The dispersion parameter of the NB distribution was fixed at 5.0 for all nodes.

Data were simulated using logic sampling to preserve the structure implied by the DAG (Koller and Friedman, 2009). For each node, the probability of generating a structural zero was determined from the values of its parents and the corresponding zero-inflation parameters. When a nonzero value was generated, it was sampled from a negative binomial distribution with parameters determined by the mean component of the model. This procedure produced datasets that exhibited both zero inflation and overdispersion, consistent with the topology of the specified DAG structure. For each of $D = 20, 30$ and 50 , we generated 10 replicate datasets and learned the network structure using the methods described below. The estimated graphs were then compared with the true underlying graph using Structural Hamming Distance (SHD; Tsamardinos et al., 2006), Structural Intervention Distance (SID; Peters and Buhlmann, 2015), True Positive Rate (TPR), and False Discovery Rate (FDR). SHD and SID were computed with the bnlearn R package (Scutari, 2010). For evaluation, we thresholded the absolute values of the entries of the learned matrices W_0, W_1 to obtain directed edges.

We compared ZICO with the state-of-the-art Greedy Equivalence Search (GES; score-based, Chickering, 2002), Max-Min Hill Climbing (MMHC; hybrid, Tsamardinos et al., 2006) and DirectLiNGAM (Shimizu et al., 2011). As for algorithms tailored to zero-inflated data, we considered ZiDAG and ZiGDAG (score-based, hyper-Poisson and NB distributions) as well as NOTEARS with a Poisson loss (continuous optimization). For GES, MMHC, DirectLiNGAM, and ZiDAG, $\log(x + 1)$ -transformed count data was used as input for the structure learning. For the other algorithms, the raw simulated count data were used as the input. We used the implementation of GES

Algorithm	TPR	FDR	Time (s)	SHD	SID	Graph model
DirectLiNGAM	0.002 (0.002)	0.965 (0.040)	108.480 (9.788)	313.500 (18.222)	2282.600 (101.654)	ER
GES	0.076 (0.019)	0.759 (0.059)	0.500 (0.081)	318.100 (21.471)	2566.300 (122.864)	ER
MMHC	0.081 (0.016)	0.671 (0.060)	1.287 (0.368)	314.100 (17.754)	2380.900 (135.685)	ER
NOTEARS	0.116 (0.029)	0.106 (0.057)	72.144 (68.673)	287.900 (16.603)	2127.100 (98.747)	ER
ZICO (NB)	0.758 (0.031)	0.479 (0.029)	48.239 (38.484)	229.500 (21.824)	1831.200 (195.047)	ER
ZICO (Poisson)	0.590 (0.053)	0.595 (0.038)	42.975 (37.211)	276.700 (32.582)	2251.700 (154.873)	ER
ZICO (ZINB)	0.780 (0.020)	0.407 (0.020)	55.643 (39.179)	180.500 (17.116)	1660.100 (164.593)	ER
ZICO (ZIP)	0.748 (0.042)	0.421 (0.037)	51.975 (38.649)	188.500 (28.321)	1792.800 (201.923)	ER
ZiDAG	0.016 (0.009)	0.507 (0.223)	789.730 (90.073)	303.300 (16.269)	2222.600 (94.768)	ER
ZiGDAG	0.100 (0.013)	0.590 (0.041)	21571.112 (1560.249)	283.200 (18.432)	2474.100 (118.722)	ER
ZiGDAG (NB)	0.102 (0.018)	0.589 (0.057)	1869.899 (343.458)	282.500 (19.086)	2456.200 (89.170)	ER
DirectLiNGAM	0.022 (0.024)	0.930 (0.062)	81.601 (0.972)	150.800 (2.394)	2435.000 (55.102)	BA
GES	0.365 (0.057)	0.580 (0.056)	0.634 (0.097)	125.000 (10.853)	2257.600 (135.318)	BA
MMHC	0.306 (0.034)	0.543 (0.044)	11.419 (8.484)	129.400 (8.959)	2328.400 (82.141)	BA
NOTEARS	0.284 (0.066)	0.220 (0.093)	118.902 (111.393)	124.000 (7.087)	2398.200 (95.381)	BA
ZICO (NB)	0.791 (0.048)	0.506 (0.043)	41.966 (33.133)	137.300 (18.815)	1212.900 (220.299)	BA
ZICO (Poisson)	0.658 (0.065)	0.495 (0.049)	41.041 (35.064)	114.100 (10.837)	1638.100 (279.596)	BA
ZICO (ZINB)	0.792 (0.038)	0.321 (0.036)	48.842 (33.577)	74.300 (8.001)	1246.800 (219.674)	BA
ZICO (ZIP)	0.760 (0.038)	0.321 (0.036)	47.724 (35.264)	76.500 (9.698)	1376.100 (223.746)	BA
ZiDAG	0.045 (0.030)	0.609 (0.145)	990.282 (132.780)	139.800 (3.765)	2451.900 (31.593)	BA
ZiGDAG	0.402 (0.059)	0.511 (0.048)	18428.821 (4741.086)	102.300 (7.558)	2264.100 (115.928)	BA
ZiGDAG (NB)	0.413 (0.041)	0.494 (0.043)	1086.489 (683.056)	100.600 (6.381)	2237.900 (119.419)	BA

Table 1: Performance comparison ($D = 50$). Values are averages over 10 replicates. The values inside parentheses are standard deviations. The best performing values are shown in bold. HP, hyper-Poisson; NB, negative binomial; ZICO: our proposal.

in the pcalg R package (Kalisch et al., 2012), and those of DirectLiNGAM and MMHC in bnlearn. The equivalence class learned by GES was replaced by its consistent DAG extension before computing SHD and SID. In this experiment, the epochs, α , and the first μ were set to 4000, 0.1, and 1, respectively. Weighted adjacency matrices were binarized at the absolute value threshold of 0.3.

The performance of various algorithms for recovering DAGs using the simulated zero-inflated data summarized in Table 1. Our ZICO proposal demonstrated comparable or superior accuracy to other approaches, with faster execution times than ZiGDAG and ZiDAG. The speed-up was most pronounced when the number of variables was large. As for structural accuracy, ZICO also yielded the lowest errors, achieved in the ZINB model with $D = 50$ and in the ER model, indicating close reconstruction of the true networks.

The superior performance of the methods based on ZINB and ZIP is expected, as these methods explicitly model the zero-inflated nature of the data. By aligning the statistical assumptions with the underlying data-generating process, they achieve higher accuracy compared with conventional approaches.

4.2. Sign and Norm-Comparison Experiment

To assess the sensitivity of ZICO to different data-generating processes, we evaluated the sign patterns between W_0 and W_1 . For each graph type $g \in \{\text{BA}, \text{ER}\}$ and dimension $D = 20$, we generated a random DAG B as described previously, fixed $N = 500$ observations, and drew edge weights from uniform ranges under different sign configurations.

Configuration	W_0low	W_0high	W_1low	W_1high	g	λ_{group}	λ_{align}	Norm	AUPRC
(-, -)	-2.0	-0.5	-2.0	-0.5	BA	0.010	0.0	none	0.826 (0.079)
(-, -)	-2.0	-0.5	-2.0	-0.5	ER	0.010	0.0	none	0.812 (0.065)
(-, +)	-2.0	-0.5	0.5	2.0	BA	0.000	0.0	none	0.325 (0.041)
(-, +)	-2.0	-0.5	0.5	2.0	ER	0.000	0.0	none	0.460 (0.125)
(+, -)	0.5	2.0	-2.0	-0.5	BA	0.001	0.1	ℓ_1	0.772 (0.091)
(+, -)	0.5	2.0	-2.0	-0.5	ER	0.010	0.1	ℓ_1	0.797 (0.043)
(+, +)	0.5	2.0	0.5	2.0	BA	0.001	0.1	ℓ_1	0.858 (0.059)
(+, +)	0.5	2.0	0.5	2.0	ER	0.000	0.1	ℓ_1	0.865 (0.042)

Table 2: Best ZICO parameter combinations for each (W_0, W_1, g) group maximizing AUPRC (W_0W_1). W_0low , W_0high , W_1low , W_1high indicate the lower and upper bounds of uniform distribution in W_0 and W_1 . The values inside parentheses are standard deviations.

We experimented with four sign configurations:

$$(\text{sign}(W_0), \text{sign}(W_1)) \in \{(+, +), (-, -), (+, -), (-, +)\}.$$

Unless otherwise stated, $(+, -)$ denotes $W_0 > 0$ (zero link) and $W_1 < 0$ (count link), and $(-, +)$ denotes the opposite. For example, in $(+, +)$, parents make zeros more likely, but conditional on being nonzero, counts are larger. This yields many zeros with occasionally large positive counts.

We also compare three ways of coupling W_0 and W_1 : 1) alignment with the Frobenius norm, at $\lambda_{\text{align}} \in \{0, 0.1, 1\}$; 2) alignment with an elementwise ℓ_1 norm, at the same λ_{align} ; 3) a combined approach that aggregates the two matrices via elementwise ℓ_2 pooling ($\widetilde{W} = \sqrt{W_0^{\circ 2} + W_1^{\circ 2} + \varepsilon}$) and enforces acyclicity on \widetilde{W} . Furthermore, we vary $\lambda_{\text{group}} \in \{0, 0.001, 0.01\}$.

We evaluate couplings using the area under the precision-recall curve (AUPRC) for the combined W_0 and W_1 , based on the edge ranking obtained from the weighted adjacency matrix. We generated five data replicates for each experimental setting.

The results of the experiments are summarized in Table 2. The optimal tuning parameter values for ZICO varied across the four sign configurations. Still, we found that the separate acyclicity plus light ℓ_1 alignment ($\lambda_{\text{align}} = 0.1$) when the W_0 is positive, yields the best AUPRC. Heavy alignment and large group penalties consistently underperformed. Notably, the $(-, +)$ combination performed markedly worse than other choices across all experimental settings. We considered the reason to be a mismatch between data generation and likelihood, and the improvements there likely require changes beyond the model architecture or hyperparameters rather than stronger regularization.

4.3. Simulations for different support for W_0 and W_1

To decouple patterns between the zero-inflation and count components and characterize the effect of the alignment penalty term, we partitioned the edge set of the DAG into two support masks with a user-specified overlap fraction ρ , yielding \mathbf{M}_0 for the zero-inflation mechanism and \mathbf{M}_1 for the mean model. Edge weights W_0 and W_1 were sampled on their respective supports, \mathbf{M}_0 and \mathbf{M}_1 . As zero-inflation and count processes may not hold in all contexts, we varied $\rho \in \{0, 0.25, 0.5, 0.75, 1\}$ to simulate how the proposed algorithm performs under different alignment penalties and λ_{align} . We

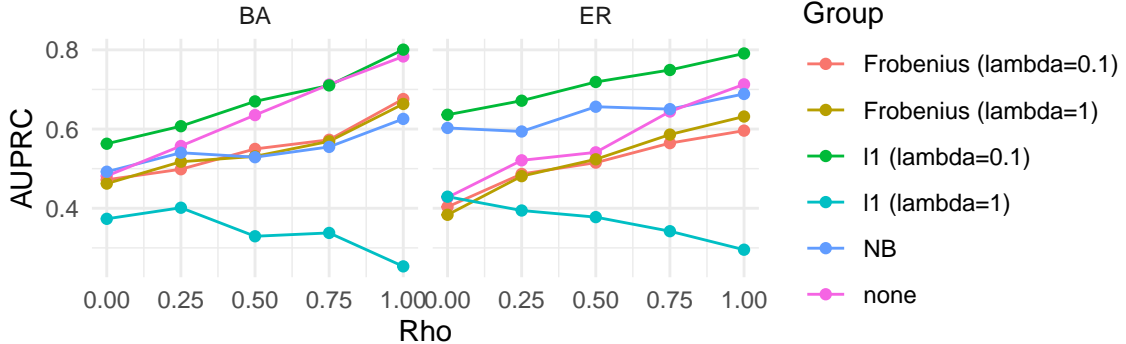


Figure 1: The AUPRC across multiple overlap levels ρ . At higher overlap, the no alignment setting achieves performance comparable to the alignment settings, whereas at lower overlap, introducing a light alignment term can improve performance. Note that AUPRC for W_1 is reported for NB model.

evaluated $g \in \{\text{BA}, \text{ER}\}$ and $(+, +)$ for generating data under the ZINB model in this experiment. We generated five data replicates for each condition.

Under $(+, +)$, the alignment strength directly applied to the chosen norm yields a ρ -dependent trade-off. When the overlap is low, a light ℓ_1 alignment is the best choice. In contrast, no alignment with the coupled acyclicity rose steadily with ρ and performed comparable to the alignment setting at high overlap in our experiments, indicating that when the common backbone between W_0 and W_1 is strong, forcing acyclicity to coupled adjacency matrix can be beneficial, yielding comparable performance in the $(+, +)$ case under the BA model (Figure 1).

4.4. Simulated SCT Data

Bayesian networks have been widely applied to GRN inference from transcriptomics data obtained from microarray and RNA-seq technology (Imoto et al., 2003). We conducted an evaluation using scMultiSim, a state-of-the-art SCT data simulator that supports GRN simulations (Li et al., 2025).

We first generated random DAGs under the BA model with the expected number of three neighbours per node, and assigned effect sizes to each edge by sampling from a $U(1, 5)$. We then generated cell-count data with $N = 500$ cells, trained networks on them with ZICO, evaluated the learned DAGs accuracy. As a means of comparison, we also performed GRN inference using GENIE3 (Huynh-Thu et al., 2010), GRNBoost2 (Moerman et al., 2019), LEAP (Specht and Li, 2017), SINCERITIES (Papili Gao et al., 2018), NOTEARS (Zheng et al., 2018). For GENIE3, GRN-Boost2, and ZICO, we used the raw count data. For the other data, a $\log(x + 1)$ transformation was applied before the inference. We used L2 loss in NOTEARS inference. Pseudo-time ordering, which is necessary for some algorithms, was calculated using the slingshot R package (Street et al., 2018). As most GRN inference methods do not explicitly produce a DAG, accuracy was evaluated using the AUPRC ratio, defined as the ratio of the AUPRC value to that obtained when using random edges.

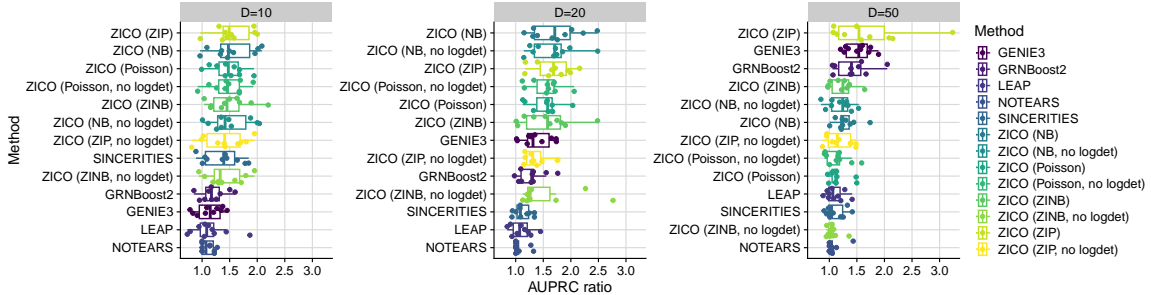


Figure 2: Performance in recovering transcriptomic regulatory relationships, assessed by the AUPRC ratio (AUPRC/AUPRC_{random}). Algorithms are ordered by the median values.

Whether the individual molecular identifier count data are zero-inflated is a matter of debate (Cao et al., 2021). This can be modelled naturally by omitting the W_0 term in (1), thus reducing it to an NB or Poisson regression NLL. Therefore, in this experiment, we used NB, Poisson, ZINB, and ZIP models, and computed AUPRC using the absolute values of the W_1 coefficient matrix in the NB and Poisson models and the combined W_0 and W_1 in the ZINB and ZIP models. We chose the alignment penalty to be the ℓ_1 norm with $\lambda_{\text{align}} = 0.1$, which performed best in earlier (+, -) experiments where the zero link and the count link act in opposite directions. In SCT data, such a configuration is consistent with the empirical behavior of dropout stochastic detection failures, which are more likely at low true expression, so that higher dropout co-occurs with lower observed positive counts (Kharchenko et al., 2014).

The results of reverse engineering GRNs using ZICO are shown in Figure 2 along with those from other commonly used directed GRN inference methods. Overall, the assessment using the AUPRC ratio relative to random prediction shows that the performance in recovering GRN is generally low, consistent with previous studies. ZICO achieved results comparable to or better than other commonly used methods for GRN inference. We hypothesize that the reason is that ZICO provides a close surrogate for the Poisson–Beta models used in the scMultiSim. DAG constraints, which are absent from other GRN inference algorithms, could also enhance performance; the ablation of the log-determinant term degraded performance in some settings.

In addition, we performed dropout simulation experiments on the clean count data. Following previous studies (e.g., Dibaeinia and Sinha, 2020), we introduced expression-dependent dropout into the clean data. We then evaluated ZICO with both ZINB/ZIP and NB/Poisson models on the resulting datasets, comparing their performance using the same AUPRC-ratio metric.

Specifically, we applied a probabilistic dropout to an input count matrix $X \in \mathbb{N}_0^{n \times d}$ and returned $Y = X \circ B$. First, we performed the elementwise transformation $z_{ij} = \log(x_{ij} + 1)$ and pooled $\{z_{ij}\}$ across all entries. Let $m = \text{Percentile}_q(\{z_{ij}\})$ be the q -th percentile that defines the threshold of a logistic function. For each entry, the retention probability is $p_{ij} = \{1 + \exp[-\alpha(z_{ij} - m)]\}^{-1}$ with slope $\alpha > 0$; larger x_{ij} yield larger z_{ij} and hence larger p_{ij} . We then sampled an independent Bernoulli mask $b_{ij} \sim \text{Bernoulli}(p_{ij})$ for all (i, j) and obtained the dropout-perturbed output by $Y = X \circ B$ with $B = (b_{ij})$. The percentile q controls the location of the threshold. We used $\alpha = 1$ and $q = 65$ in the experiment.

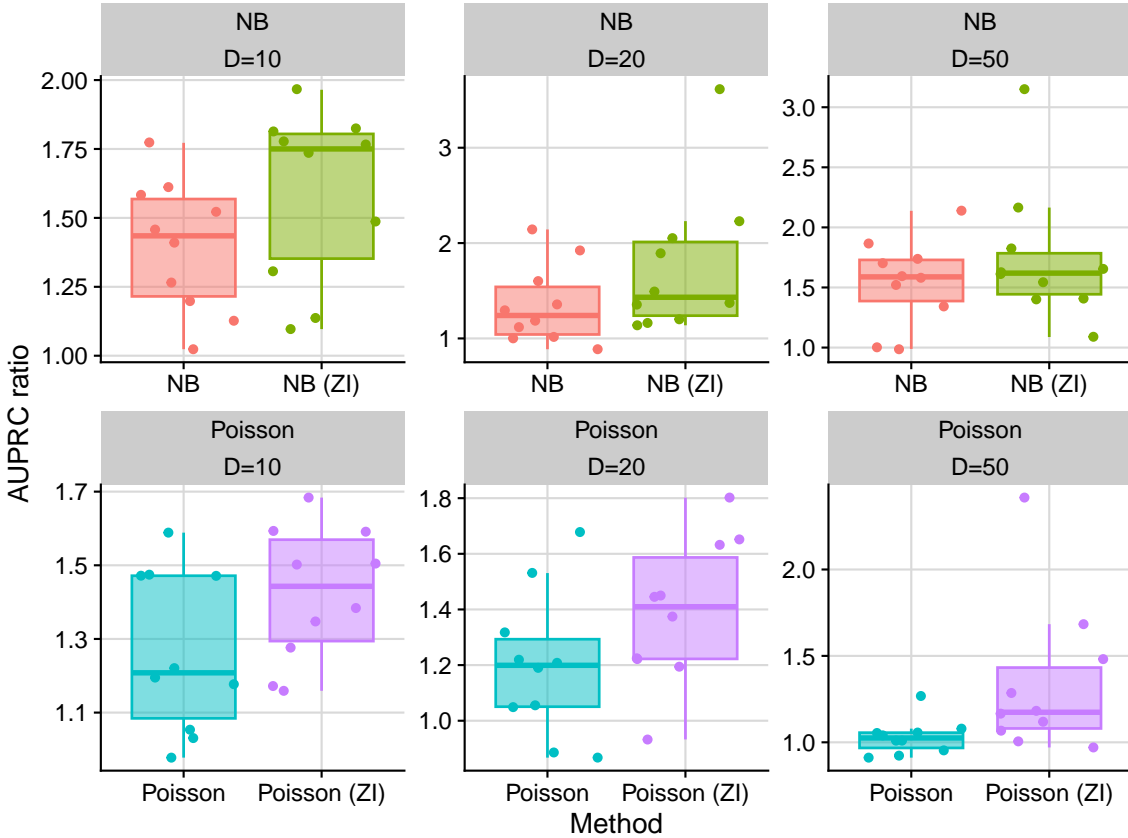


Figure 3: Comparison of the performance of recovering GRN from the count data applied dropout simulation. The boxplot comparing ZINB, ZIP, NB, and Poisson models assessed by the AUPRC ratio (AUPRC/AUPRC_{random}) is shown.

The results are shown in Figure 3. The ZINB and ZIP approaches, which incorporate W_0 , consistently achieved higher AUPRC ratios across all D values than the NB and Poisson models. This suggests that estimators that account for zero inflation are advantageous when estimating DAG from SCT data with dropout events.

4.5. Evaluation Environment

The proposed ZICO is implemented in PyTorch. All code is available from <http://www.github.com/noriakis/ZICO>. Training was carried out on the supercomputer SHIROKANE using PyTorch 2.6.0 (Paszke et al., 2019). We used ggplot2 for data visualization. The performance statistics were calculated using scikit-learn (Pedregosa et al., 2011). The supercomputing resource was provided by the Human Genome Centre, the Institute of Medical Science, the University of Tokyo.

5. Conclusions

We developed ZICO, an accurate and efficient algorithm to learn DAGs from zero-inflated count data through continuous optimization. Compared to existing methods, ZICO scales to larger numbers of variables, making it practical in real-world settings such as GRN inference from SCT data.

Continuous optimization methods have been criticized for issues with varsorability (Reisach et al., 2021). Because the variance is not estimated independently from the mean but determined by the underlying distributional form, this issue should not be relevant in this setting. Nevertheless, a theoretical analysis of identifiability and potential biases under different data-generating mechanisms remains an important direction for future work.

Reverse engineering GRN from SCT data has been reported to be challenging in several works (Chen and Mar, 2018; Dibaeinia and Sinha, 2020). Zero-inflation is also still debated in SCT data; the ZIP/ZINB components in the model help with clearly zero-inflated data. They are otherwise over-parameterized (Cao et al., 2021), as we have shown using simulated SCT data: NB models may then outperform zero-inflated models. In practice, this suggests that model choice should account for both empirical characteristics of the data and prior knowledge of the underlying measurement technology. ZICO can naturally accommodate such choices, since the same optimization scheme can be coupled with different count distributions, including NB and Poisson variants. As a limitation, our empirical evaluation focused on explicitly acyclic structures; feedback loops and other non-DAG regulatory motifs, which are common in biology, and are not captured by the current formulation.

6. Acknowledgements

This study is partially supported by Takeda Science Foundation, JSPS KAKENHI 25K21331; and grant K25-2170 from the International Joint Usage/Research Center, the Institute of Medical Science, the University of Tokyo.

References

- K. Bello, B. Aragam, and P. Ravikumar. DAGMA: Learning DAGs via M-Matrices and a Log-Determinant Acyclicity Characterization. In *Proceedings of the 36th International Conference on Neural Information Processing Systems*, pages 8226–8239, 2022.
- Y. Cao, S. Kitanovski, R. Küppers, and D. Hoffmann. UMI or Not UMI, That Is the Question for ScRNA-Seq Zero-Inflation. *Nature Biotechnology*, 39(2):158–159, 2021.
- S. Chen and J. C. Mar. Evaluating Methods of Inferring Gene Regulatory Networks Highlights Their Lack of Performance for Single Cell Gene Expression Data. *BMC Bioinformatics*, 19(1):232, 2018.
- D. M. Chickering. Optimal Structure Identification With Greedy Search. *Journal of Machine Learning Research*, 3:507–554, 2002.
- J. Choi and Y. Ni. Model-Based Causal Discovery for Zero-Inflated Count Data. *Journal of Machine Learning Research*, 24(200):1–32, 2023.

- J. Choi, R. Chapkin, and Y. Ni. Bayesian Causal Structural Learning with Zero-Inflated Poisson Bayesian Networks. In *Proceedings of the 34th International Conference on Neural Information Processing Systems*, pages 5887–5897, 2020.
- G. Csárdi and T. Nepusz. The igraph Software Package for Complex Network Research. *Interjournal, Complex Systems*:1695, 2006.
- T. Cui and T. Wang. A Comprehensive Assessment of Hurdle and Zero-Inflated Models for Single Cell RNA-Sequencing Analysis. *Briefings in Bioinformatics*, 24(5):bbad272, 2023.
- P. Dibaeinia and S. Sinha. SERGIO: A Single-Cell Expression Simulator Guided by Gene Regulatory Networks. *Cell Systems*, 11(3):252–271.e11, 2020.
- V. A. Huynh-Thu, A. Irrthum, L. Wehenkel, and P. Geurts. Inferring Regulatory Networks From Expression Data Using Tree-Based Methods. *PLoS One*, 5(9):e12776, 2010.
- S. Imoto, T. Higuchi, T. Goto, K. Tashiro, S. Kuhara, and S. Miyano. Combining Microarrays and Biological Knowledge for Estimating Gene Networks via Bayesian Networks. *Proceedings. IEEE Computer Society Bioinformatics Conference*, 2:104–113, 2003.
- M. Kalisch, M. Mächler, D. Colombo, M. H. Maathuis, and P. Bühlmann. Causal Inference Using Graphical Models with the R Package pcalg. *Journal of Statistical Software*, 47(11):1–26, 2012.
- P. V. Kharchenko, L. Silberstein, and D. T. Scadden. Bayesian Approach to Single-Cell Differential Expression Analysis. *Nature Methods*, 11(7):740–742, 2014.
- D. Koller and N. Friedman. *Probabilistic Graphical Models: Principles and Techniques*. MIT Press, 2009.
- H. Li, Z. Zhang, M. Squires, X. Chen, and X. Zhang. scMultiSim: Simulation of Single-Cell Multi-Omics and Spatial Data Guided by Gene Regulatory Networks and Cell-Cell Interactions. *Nature Methods*, 22(5):982–993, 2025.
- I. Loshchilov and F. Hutter. Decoupled Weight Decay Regularization. In *Proceedings of the International Conference on Learning Representations*, pages 1–11, 2019.
- A. McDavid, R. Gottardo, N. Simon, and M. Drton. Graphical Models for Zero-Inflated Single Cell Gene Expression. *The Annals of Applied Statistics*, 13(2):848–873, 2019.
- T. Moerman, S. Aibar Santos, C. Bravo González-Blas, J. Simm, Y. Moreau, J. Aerts, and S. Aerts. grnboost2 and Arboreto: Efficient and Scalable Inference of Gene Regulatory Networks. *Bioinformatics*, 35(12):2159–2161, 2019.
- A. Nazaret, J. Hong, E. Azizi, and D. Blei. Stable Differentiable Causal Discovery. In *Proceedings of the 41st International Conference on Machine Learning*, pages 37413–37445, 2024.
- I. Ng, A. Ghassami, and K. Zhang. On the Role of Sparsity and DAG Constraints for Learning Linear DAGs. In *Proceedings of the 34th International Conference on Neural Information Processing Systems*, pages 17943–17954, 2020.

- N. Papili Gao, S. M. M. Ud-Dean, O. Gandrillon, and R. Gunawan. SINCERITIES: Inferring Gene Regulatory Networks From Time-Stamped Single Cell Transcriptional Expression Profiles. *Bioinformatics*, 34(2):258–266, 2018.
- G. Park and G. Raskutti. Learning Large-Scale Poisson DAG Models Based on Overdispersion Scoring. In *Proceedings of the 29th International Conference on Neural Information Processing Systems - Volume 1*, pages 631–639, 2015.
- A. Paszke, S. Gross, F. Massa, A. Lerer, J. Bradbury, G. Chanan, T. Killeen, Z. Lin, N. Gimelshein, L. Antiga, A. Desmaison, A. Köpf, E. Yang, Z. DeVito, M. Raison, A. Tejani, S. Chilamkurthy, B. Steiner, L. Fang, J. Bai, and S. Chintala. Pytorch: An Imperative Style, High-Performance Deep Learning Library. In *Proceedings of the 33rd International Conference on Neural Information Processing Systems*, pages 8026–8037. 2019.
- F. Pedregosa, G. Varoquaux, A. Gramfort, V. Michel, B. Thirion, O. Grisel, M. Blondel, P. Prettenhofer, R. Weiss, V. Dubourg, J. Vanderplas, A. Passos, D. Cournapeau, M. Brucher, M. Perrot, and E. Duchesnay. Scikit-Learn: Machine Learning in Python. *Journal of Machine Learning Research*, 12:2825–2830, 2011.
- J. Peters and P. Bühlmann. Structural Intervention Distance (SID) for Evaluating Causal Graphs. *Neural Computation*, 27:771–799, 2015.
- A. G. Reisach, C. Seiler, and S. Weichwald. Beware of the Simulated DAG! Causal Discovery Benchmarks May Be Easy to Game. In *Proceedings of the 35th International Conference on Neural Information Processing Systems*, pages 27772–27784, 2021.
- M. Schmidt, A. Niculescu-Mizil, and K. Murphy. Learning Graphical Model Structure Using L1-Regularization Paths. In *Proceedings of the 22nd National Conference on Artificial Intelligence - Volume 2*, pages 1278–1283, 2007.
- M. Scutari. Learning Bayesian Networks with the bnlearn R Package. *Journal of Statistical Software*, 35(3):1–22, 2010.
- S. Shimizu, T. Inazumi, Y. Sogawa, A. Hyvärinen, Y. Kawahara, T. Washio, P. O. Hoyer, and K. Bollen. DirectLiNGAM: A Direct Method for Learning a Linear Non-Gaussian Structural Equation Model. *Journal of Machine Learning Research*, 12(33):1225–1248, 2011.
- A. T. Specht and J. Li. LEAP: Constructing Gene Co-Expression Networks for Single-Cell RNA-Sequencing Data Using Pseudotime Ordering. *Bioinformatics*, 33(5):764–766, 2017.
- K. Street, D. Risso, R. B. Fletcher, D. Das, J. Ngai, N. Yosef, E. Purdom, and S. Dudoit. Slingshot: Cell Lineage and Pseudotime Inference for Single-Cell Transcriptomics. *BMC Genomics*, 19(1):477, 2018.
- I. Tsamardinos, L. E. Brown, and C. F. Aliferis. The Max-Min Hill-Climbing Bayesian Network Structure Learning Algorithm. *Machine Learning*, 65(1):31–78, 2006.
- S. Yu, M. Drton, and A. Shojaie. Directed Graphical Models and Causal Discovery for Zero-Inflated Data. In *Proceedings of the Second Conference on Causal Learning and Reasoning*, pages 27–67, 2023.

- X. Zheng, B. Aragam, P. Ravikumar, and E. P. Xing. DAGs with No Tears: Continuous Optimization for Structure Learning. In *Proceedings of the 32nd International Conference on Neural Information Processing Systems*, pages 9492–9503, 2018.